Turkish Journal of Electromechanics and Energy
ISSN: 2547-975X
Vol:7, No:2, Page 41-47 (2022)
https://www.scienceliterature.com

Turkish Journal of Electromechanics & Energy
an international open access journal

Speed control of MT2240A DC motor with an observer-based linear quadratic regulator

Ömer Kasım[1, *]

[1] Department of Electrical and Electronics Engineering, Simav Technology Faculty, Kütahya Dumlupınar University, Kütahya, Turkey

ARTICLE INFO

***Article Type*:**
Selected Research Article [c]

Article History:
Received: 27 September 2021
Revised: 20 January 2022
Accepted: 9 March 2022
Published: 30 March 2022

Editor of the Article:
M. E. Şahin

Keywords:
DC motor speed control, Observed based linear quadratic regulator, PID controller, Closed-loop response

ABSTRACT

The design of Direct Current (DC) motor speed control, which is preferred due to its high torque in industrial applications, is a challenging task. The Linear Quadratic Regulator (LQR) controller ensures the well-controlled behavior of the system by minimizing the error in speed control. This can only be achieved if the rank of the controllability matrix is maximum. The rank value of the MT2240A DC motor used in the study is calculated as one. In this study, the LQR controller enriched with an observed-based design was used to overcome this problem. In the experiments, the transient and steady-state behavior metrics of the speed control were compared in the simulation environment of the plant controlled by the Proportional Integral Derivative (PID) controller, and the closed-loop response of the plant to determine the efficiency of the presented design. It was observed that the LQR controller has an optimum response with more effective transient and steady-state responses compared to the PID controller. This result enabled the LQR controller design, which was inadequate in terms of controllability, and the results is proved that the observation-based LQR controller dynamically responded better.

Cite this article: Ö. Kasım, "Speed control of MT2240A DC motor with an observer-based linear quadratic regulator," *Turkish Journal of Electromechanics & Energy*, 7(1), pp.41-47, 2022.

1. INTRODUCTION

Direct Current (DC) motors are used in industrial applications involving position and speed control. The advantages of DC motors are lower power consumption and high torque characteristics compared to AC motors [1]. Thanks to these features, it is preferred in applications requiring different speed range variations and high torque [2]. A proportional Integral Derivative (PID) controller is generally preferred in these applications. K_p, K_i, and K_d parameters in the structure of the PID controller are adjusted manually based on the knowledge of the technicians [3]. For more successful control, schemas, these parameters are optimized using methods such as the Ziegler-Nicholes method, PID tuner, and ant colony algorithm [4]. The best settling time of the DC motor and the least overshot are targeted with these optimization techniques [5]. Since industrial applications generally contain non-linear characteristics, linear controllers fail to give good dynamic responses when changing states. This results in large overshoot and long settling times [6]. Therefore, there is a need for the Linear Quadratic Regulator (LQR) control technique that can optimize the control solution [7]. The main focus of this article is to control the DC motor's speed control system's input voltage with LQR.

In speed control with LQR, the cost function, which includes the weights of the inputs and situations, is optimized to obtain transient and steady-state performances [8, 9]. High dimensionality and numerical stiffness can be alleviated with this optimization [10]. However, this solution is obtained by necessarily equaling the individual perturbation parameter to zero [11]. In addition, harmonic distortions and individual perturbation negatively affect accuracy in nonlinear DC motor speed control [12]. Although there are different approaches to the solution of this problem, the problem is optimized by using an observer-based control scheme together with the LQR controller [13, 14].

Wang et al. proposed a linear quadratic regulator (LQR) optimized backpropagation neural network (BPNN) PI controller, called LN-PI, for speed control of a brushless direct current (BLDC) motor. Performance analysis of the proposed controller is presented under Matrix Laboratory (MATLAB) / Simulink for comparison with traditional PI controller, neural network PI controller, and LQR optimized PI controller. As a result of the experiments, the proposed controller improves the response speed effectively, reduces the steady-state error, and improves the anti-interference feature [15]. Ahmad et al. developed an optimal control for the quadcopter's position and yaw control based on the linear quadratic regulator (LQR). Quadcopter dynamics, their behavior has been described in three-dimensional spaces. The improved LQR based controller was

[c] Initial version of this article was presented in the International Conferences on Engineering, and Natural Sciences (IOCENS'21) held on July 5-7, 2021, in Gümüşhane, TURKEY. It was subjected to a peer-review process before its publications

*Corresponding author e-mail: omer.kasim@dpu.edu.tr

used for speed control of motors in propellers [16]. Maghfiroh et al. tried to use the LQR controller to reduce energy consumption in the DC motor control system. The test results show that the LQR method has lower energy consumption and a better Integral Square Error (ISE) performance compared to the PID controller [17]. Masroor et al. presented an innovative method to address the synchronous speed problem in DC motors using the leading follower multi-factor system (MAS) consensus algorithm with linear quadratic regulator control. From the MAS perspective, each chopper powered by the DC motor is considered to be the only agent connected over the fixed and undirected network. In this work, the common Lyapunov function is used to ensure key system stability. To verify the proposed method, the simulation results are presented using MATLAB, taking into account the application of the load to the motors and without load [18]. Bharti et al. proposed a switched LQR speed controller for a linear DC motor plant model and compared transient responses and steady-state responses with a cascade controller for the same linear DC motor plant model [19]. Sharma proposed an alternative technique for the speed of the DC motor via a nonlinear controller designed by an artificial neural network (ANN) [20]. Aravind et al. designed an LQR controller for DC motor speed control [21].

In this study, the effect of the LQR approach on speed control of a Baldor MT-2240A model DC motor was presented in a simulation environment. The mathematical model of the plant was obtained with the datasheet parameters of the DC motor. The analysis performed by connecting the PID controller optimized with the PID tuner in the MATLAB program to this model was tested in comparison with the LQR controller presented in the study. The LQR controller, which was designed based on the observer, which is effective against the speed control of the DC motor, which is a nonlinear control, provided more successful results in the settling time and overshoot criteria. This result has proven the effective contribution of the LQR controller, especially in applications where speed control of the DC motor is important.

2. MATERIAL AND METHODS

2.1. Proposed Method

The rank value for controllability must be obtained as much as the size of the A matrix for the LQR controller used in the speed control of the DC motor. The controllability rank value of the DC motor used in this study can only be found as one. It is not possible to design an LQR controller with this value. For this reason, with the observer model design, both the LQR controller can be designed independently of controllability, and the motor can catch the desired reference speed value with the feedback performed according to the results obtained from the observation. The LQR controller was designed in the simulation environment with the system design as shown in Figure 1. The plant settled at the reference value by using the *K* gain values and the contribution of the *L* value. As a result, the most optimum solution was obtained by running multiple simulations with the LQR controller.

2.2. State Space Model of Control System for a DC Motor

While a DC motor is modeled mathematically, it is handled in two parts electrical and mechanical parts. The electrical part is generally called armature and consists of a resistor and coil. The mechanical part starts to rotate with the stimulation in the mechanical part with the stress applied to this part. In the mechanical part, there is inertia, opposing EMF, and torque constant parameters of the motor [22]. In the model proposed by Isermann, it is accepted as a linear converter that converts input motor current into torque output [23]. The input voltage is changed by a controller with a constant voltage drop in brush and rotor resistance to control the angular velocity. In general, inductance (*L*) depends on the motor current that creates the driving torque. When this block diagram is designed with the state-space model, the open-loop model in Figure 1 is obtained. An open-loop plant is obtained with the state-space model's *A*, *B*, *C*, and *D* matrices [24].

Armature-controlled DC motor consists of two parts in mathematical modeling. These are models of electrical and mechanical parts. Differential equations are used to obtain these models. The mechanical part of the armature-controlled DC motor is expressed as in Equation (1).

$$J.\frac{d\omega(t)}{dt} + B.\omega(t) = T_m(t) \tag{1}$$

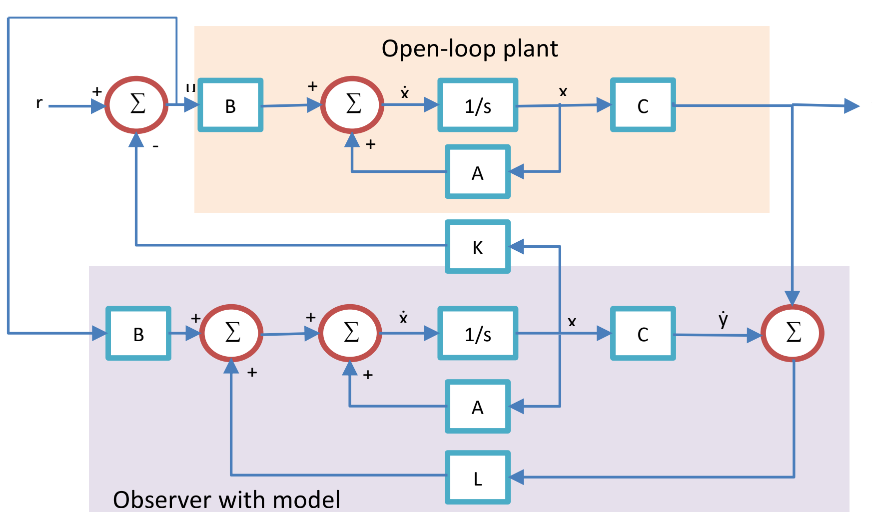

Fig. 1. Observed based LQR controller with DC motor speed control architecture.

In Equation (1), J denotes a moment of inertia and, B denotes viscous dumping. The electrical part of the DC motor is expressed by Equation (2).

$$L.\frac{di_a(t)}{dt} + R.i_a(t) = v_a(t) - v_b(t) \quad (2)$$

In Equation (2), R_a is the armature resistance and L_a is the armature inductance. With the voltage to be applied to the armature part of the motor, the mechanical movement of the motor is realized. In addition, v_a denotes the armature voltage, while v_b denotes the back electromotive force voltage. Conversions between the mechanical part and the electrical part are mathematically provided by the coefficients K_e and K_t. The relationship K_e between speed and voltage and the coefficient K_t between torque and current is expressed by Equation (3).

$$v_b = K_e.\omega(t), T_m(t) = K_t.i_a(t) \quad (3)$$

An observer-based design requires a state-space model. The state-space model enables time-dependent analysis. Equation (4) is obtained when using the given Equation (1), Equation (2), and Equation (3) to switch to the state-space model. In addition, other parameters of the motor used in the study are continuous stall torque is 0.21, the continuous current is 2.05 *A*, peak torque is 1.4 *Nm*, peak current is 12.3 *A*, voltage constant is 12 *V*.

The A, B, C, and D matrices of the DC motor model designed with the state-space model are presented in Equation (4). These matrices are obtained with the DC motor parameters used in this study and presented in Table (1).

$$A = \begin{bmatrix} 0 & 1 & 0 & 0 \\ 0 & 0 & 1 & 0 \\ 0 & \frac{R}{L} & 0 & \frac{K_t}{J} \\ 1 & -\frac{K_e}{L} & 0 & -\frac{b}{J} \end{bmatrix}, B = \begin{bmatrix} 0 & 0 \\ \frac{1}{L} & 0 \\ 0 & 0 \\ 0 & -\frac{1}{J} \end{bmatrix}, \quad (4)$$

$$C = \begin{bmatrix} 0 & 1 & 0 & 0 \\ 0 & 0 & 0 & 1 \end{bmatrix}, D = [0]$$

Table 1. Physical parameters of the DC motor model.

Parameters	*Descriptions*	*Unit*	*Values*
V_a	Input voltage	Volt	R(s)
ω	Angular velocity of the shaft	Rad/s	C(s)
R	Armature resistance	Ohm	4Ω
L	Armature inductance	Henry	7.7mH
J	Moment of inertia	Kg/m2	0.35
K_t	Torque constant of the motor	Nm/Amp	0.115
K_e	Back EMF constant	V/rad/s	0.115

Before the LQR is applied to the controller, the rank value obtained with the controllability of the system should be four. For this reason, when the controllability of the plant is inspected, the controller design that can meet the desired requirements has become possible. The poles of the system were obtained as -0.0094 + 0.0000i, 0.0047 + 72.0750i, 0.0047 -72.0750i and 1.0000 + 0.0000i, respectively.

2.3. Linear Quadratic Regulator

The LQR controller is designed using a state-space model. In this design, Q and R weight matrices are obtained. Position and speed control is provided with the cost function obtained with the content of these matrices. In LQR for a controllable linear time-invariant (LTI) system, the optimal control signal is defined by solving the algebraic Riccati equation [25]. This study used the LQR controller, which is designed based on an integrator and observer. The LQR controller, which is named the perfect controller, was obtained by using the integrator included in the control. The motor was ensured to fit the desired speed value. An optimal LQR controller adapted to an armature-controlled DC motor is shown in Figure 2.

The most important parameter in obtaining the optimum solution in the LQR controller is the gain matrix K gain matrix [26]. To calculate this matrix, the control input must be applied to the state-space model as in Equation (5).

$$X_0 = A.X + B.u(X(t_0)), Y = C.X + D.u(t) \quad (5)$$

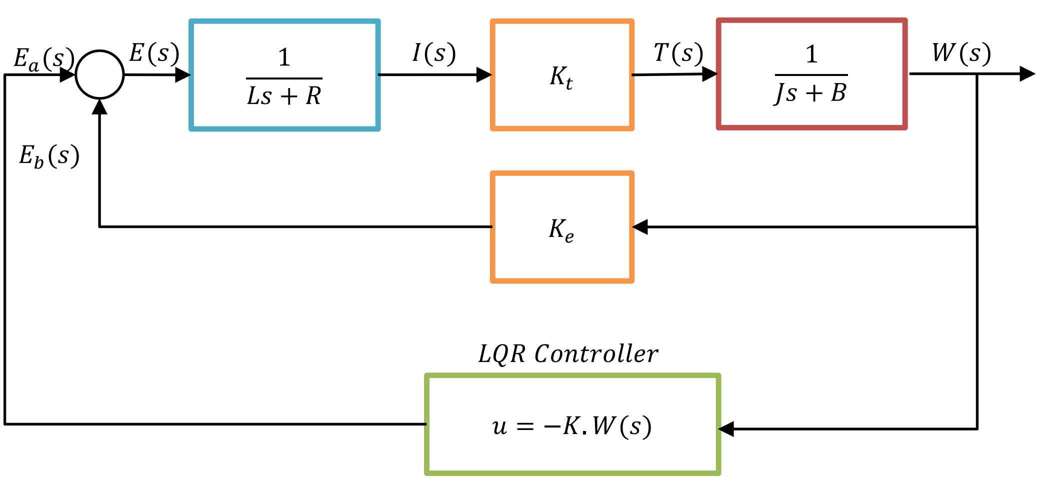

Fig. 2. Optimal LQR controller with DC motor speed control.

In Equation (5), X denotes the state vector, A state transition matrix, B control matrix, C output matrix, and $u(t)$ control signal. X_0 represents the initial values of the state vectors of the model. The Q and R matrices of the LQR controller are obtained with J notation using Equation (6).

$$J(X,u,Q,R) = \int (X^T.Q.X + u^T R.u)dt \tag{6}$$

In Equation (3), R is the weight matrix of the input variables and Q is the weight matrix of the state variables. The P value that is shown in Equation (7) is calculated by using these matrices.

$$P.A + A^T.P - P.B.R^{-1}.B^T.P + Q = 0 \tag{7}$$

Equation (4) provides the P matrix K gain values calculated by using state-space matrices and R and Q matrices. U control signal is generated with the K matrix obtained by multiplying the RBP matrices in Equation (8).

$$K = R^{-1}.B^T.P, u(t) = -K.X(t) \tag{8}$$

3. RESULTS AND DISCUSSION

The A, B, C, and D matrices of the state-space model of the DC motor used in the study are obtained as in Equation (1). The K gain matrix values were obtained as 44.7213, 49.0701, and 0.1762 respectively with the LQR controller based on the observation realized with these matrices. In this study, the speed control of the DC motor was designed with an observed-based LQR controller. When the DC motor was operated in a closed loop without using the LQR controller, a very long residence time was obtained. Although there was no overshoot, the plant settled at the reference value with an error of almost 15%. The state variables of the system are presented in four matrices in Table 2. The relationship between each interconnected state is expressed as A, B, and C in Table 2. In this case, the transfer function for the compensator obtained was $44.72/s$.

The motor simulated by perching with the PID tunnel effectively reached the reference value. A little overrun and fast settling time was provided by the PID controller. In the experiment with the proposed controller, the motor reached the reference input with a very small exceeding and a very fast settling time compared to the PID controller. Experimental results for all three conditions are expressed in Figure 3. The effective result has been achieved with the LQR controller.

Table 2. Observer states of the proposed method.

Parameters	*States*	X_1	X_2	X_3
A	X_1	-0.002	-787.8	-11.43
	X_2	18.67	-5198	0
	X_3	0	89.44	0
B	U_1	0	0	8
	U_2	0	785.1	0
	U_3	0	2.821	0
	U_4	2	0	0
C	Y_1	1.429	1	0
	Y_2	0	0	1
	Y_3	0	0	0

According to the unit-step input response performed in the experiments, the closed-loop response is compared to the PID controller and the observed-based LQR controller, whose gain coefficients K_p, K_i, and K_d are tested by the PID tuner. From the simulation results, it is seen that the LQR controller gives a good optimal response with better transient and steady-state behavior. The parameters of control responses are presented in Table 3. According to these results, a successful result was obtained in terms of rising time, settling time, and peak amount.

Similar studies in the literature showed that the LQR controller was optimized with Q and R matrices [19, 27, 28]. The rank of the controllability matrix should be four for the design in this study to be able to control the speed of the DC motor with these matrices [29]. Since the controllability rating of the Baldor brand DC motor used in this study is one, it is not possible to get results with this solution. If even one of the columns of the Q matrix is zero, the LQR check is impossible. In the solution to this problem, an observational controller design was preferred. With this design, the speed control of the motor used in this study could be controlled by LQR based on observation over K. The optimum solution was obtained in the experiment with the PID tuner function presented in the MATLAB software [30]. A more successful result was obtained from the PID optimization offered with the LQR controller.

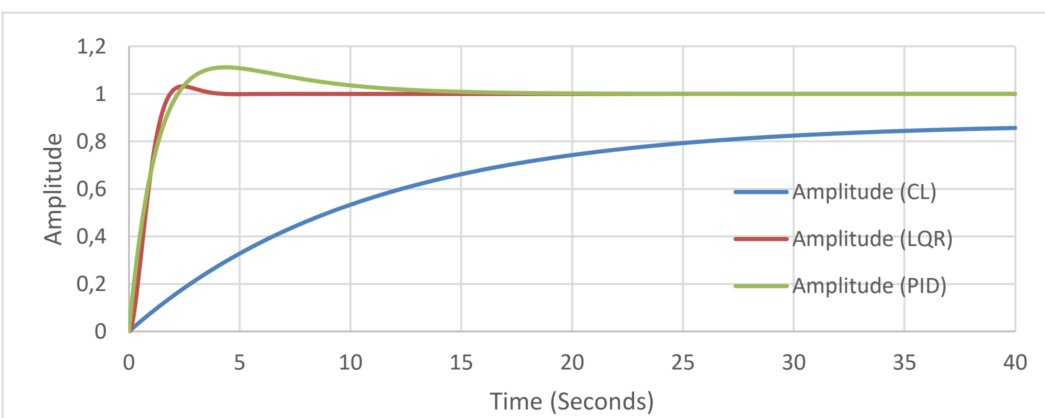

Fig. 3. Unit step input response of the closed-loop (CL) plant, PID controlled plant, and observer-based LQR controlled plant.

In addition, in the results of the analysis, the ramp input and the system sides against a periodic noise with a certain frequency were also examined. The system responses according to the ramp input of the closed-loop model with PID controller and the models with LQR controller applied in this study are presented in Figure 4. The LQR controller was found to be successful in responding faster to ramp input. In Figure 5, the model with sine input versus LQR controller has been proven as a result of experiments as having less phase shift and system response closest to the highest amplitude.

Table 3. Performance metrics of the methods.

Parameters	*CL*	*LQR*	*PID*
Rise Time	23.4674	1.1743	1.577
Settling Time	41.7871	3.0406	12.1261
Settling Min	0.7936	0.9084	0.9043
Settling Max	0.8774	1.0319	1.112
Overshoot	0	3.1911	11.1984
Undershoot	0	0	0
Peak	0.8774	1.0319	1.112
Peak Time	112.6458	2.4389	4.3195

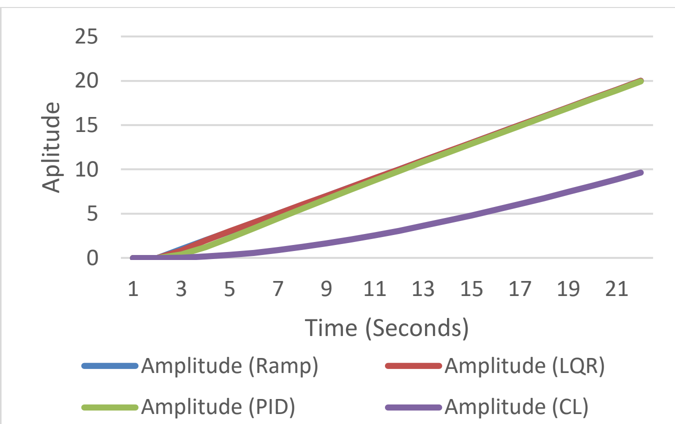

Fig. 4. Unit ramp input response of the closed-loop plant, PID controlled plant, and observer-based LQR controlled plant.

Generally, the PID controller is used in the control of the Baldor brand DC motor, which is operated as a result of simulation in the study. When the parameters of this controller are selected appropriately, it gives good results [31, 32, 33]. The Ziegler-Nicholes method in parameter selection allows mathematical calculation. However, optimum parameter calculations can be performed by using the optimization methods in the simulation environment and running them without setting up the real system. One of the most successful of these optimization methods is the PID tuner, which is investigated by Åström et al. [34]. PID coefficients can be calculated with this algorithm. The success graph of the Baldor DC motor used in the study was obtained as a result of simulation with the PID coefficients calculated optimally with these parameters and the parametric results obtained are presented in Table 3 and Figure 3. In addition, the raw behavior of the MT2240A simulation results obtained by applying a closed-loop is also given.

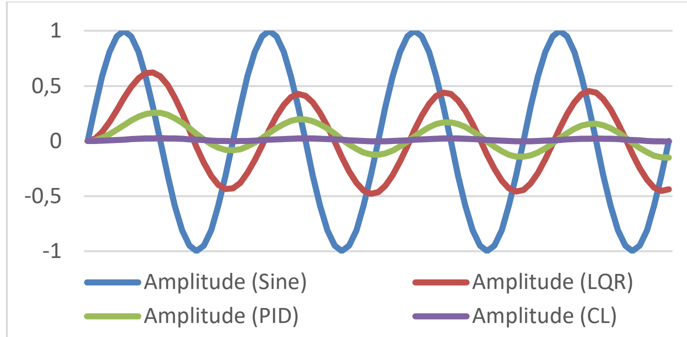

Fig. 5. The system responds to a sine wave with a period of one second and a duration of four seconds for input response of the closed-loop plant, PID controlled plant, and observer-based LQR controlled plant.

Similar studies in the literature showed that the LQR controller was optimized with Q and R matrices [18, 26, 27]. The rank of the controllability matrix should be four for the design in this study to be able to control the speed of the DC motor with these matrices [28]. Since the controllability matrix rank problem of the Baldor brand DC motor, an observational controller design was preferred. The speed control of the motor used in this study could be controlled by LQR based on observation over K with this design. The optimum solution was obtained in the experiment with the PID tuner function presented in the MATLAB software [29]. The LQR controller is generally operated with a rank of the controllability matrix in studies in the literature. However, when the controllability analysis of the DC motor used in the study is made from the state-space model, the rank matrix becomes incompatible. Therefore, it is not possible to design an LQR controller with the controllability matrix of the DC motor used in the study. It has been proven in this study that this problem can be solved with an observation-based control application. The DC motor can be controlled with a LQR controller that contains more robust results than the PID tuner by organizing the state space representation of the DC motor as in Equation (4).

4. CONCLUSION

In this paper, the speed control of the Baldor MT2210 DC motor, whose speed control is not possible with the controllability matrix rank LQR controller, was realized with an observational design. Instead of optimizing the Q and R matrices, the LQR controller was designed by adjusting the K value according to the result obtained from the observation. The experimental results of the designed design were compared with the closed-loop response and optimized PID controller results. The efficiency of the LQR controller has been proven in the simulation environment with successful results compared to the PID controller in terms of both settling time and excess amount. The reduction in settling time contributed to the rapid response, and the low amount of overshoot contributed in terms of vibration.

In future studies, the relationship between the simulation results will be revealed by real-time control of the DC motor with the LQR controller. In addition, it is planned to investigate the effects of real-time control by comparing the behavior of the observer-based controller under different loads with the PID controller.

References

[1] Ö. Cihan, M. Javadzadehkalkhoran, A. Kutlar, “Improvement of the electronic control unit for ignition and injection in a Wankel engine,” *Gümüşhane University Journal of Science and Technology*, 10(3), pp. 742-751, 2020.

[2] M. Park, Y. Kang, “Experimental verification of a drift controller for autonomous vehicle tracking: A circular trajectory using LQR method,” *International Journal of Control Automation and Systems*, 19(1), pp. 404-416, 2021.

[3] A. K. Mishra, S. R. Das, P. K. Ray, R. K. Mallick, A. Mohanty, D. K. Mishra, “PSO-GWO optimized fractional order PID based hybrid shunt active power filter for power quality improvements,” *IEEE Access*, vol.8, pp. 74497-74512, 2021.

[4] B. Jakovljević, P. Lino, G. Maione, “Control of double-loop permanent magnet synchronous motor drives by optimized fractional and distributed-order PID controllers,” *European Journal of Control*, vol. 58, pp. 232-244, 2021.

[5] M. A. Ebrahim, M. N. Ahmed, H. S. Ramadan, M. Becherif, J. Zhao, “Optimal metaheuristic-based sliding mode control of VSC-HVDC transmission systems,” *Mathematics and Computers in Simulation*, vol. 179, pp. 178-193, 2021.

[6] Y. Shin, R. Smith, S. Hwang, "Development of a model predictive control system using an artificial neural network: A case study with a distillation column," *Journal of Cleaner Production*, vol. 277, pp. 124124, 2020.

[7] D. A. Souza, V. A. de Mesquita, L.L. Reis, W. A. Silva, J. G. Batista, “Optimal lqi and PID synthesis for speed control of switched reluctance motor using metaheuristic techniques," *International Journal of Control, Automation and Systems*, 19(1), pp. 221-229, 2021.

[8] K. M. Haneesh, T. Raghunathan, “Robust Control of DFIG Based Wind Energy System Using an H∞ Controller,” *Journal of Electrical Engineering & Technology*, 16(3), pp. 1693-1707, 2021.

[9] M. A. L. Beteto, E. Assunção, M. C. M. Teixeira, E. R. P. D. Silva, L. F. S. Buzachero, R. da Ponte Caun, “Less conservative conditions for robust LQR-state-derivative controller design: an LMI approach,” *International Journal of Systems Science*, 52(12), pp. 2518-2537, 2021.

[10] S. Zimmermann, R. Poranne, R., S. Coros, “Dynamic manipulation of deformable objects with implicit integration,” *IEEE Robotics and Automation Letters*, 6(2), pp. 4209-4216, 2021.

[11] S. Mukherjee, H. Bai, H., A. Chakrabortty, “Reduced-dimensional reinforcement learning control using singular perturbation approximations,” *Automatica*, vol. 126, pp. 109451, 2021.

[12] S. K. Pandey, B. Singh, “PV–BES Microgrid System with LQR-Tuned CC–CVF-Based Control Algorithm.,” *Journal of the Institution of Engineers (India): Series B*, 102(3), pp. 585-593, 2021.

[13] P. Yu, K.Z. Liu, X. Liu, X. Li, M. Wu, M., J. She, “Analysis of equivalent-input-disturbance-based control systems and a coordinated design algorithm for uncertain systems,” *International Journal of Robust and Nonlinear Control*, vol. 31, pp. 1755–1773, 2021.

[14] T. H. Lee, W. Liang, C. W. de Silva, K. K. Tan, “Advanced Disturbance Observer-Based Failure Detection for Force Sensor,” *Springer Force and Position Control of Mechatronic Systems*, pp. 179-198, 2021.

[15] T. Wang, H. Wang, H. Hu, C. Wang, “LQR optimized BP neural network PI controller for speed control of brushless DC motor,” *Advances in Mechanical Engineering*, 12(10), pp.1687814020968980, 2020.

[16] F. Ahmad, P. Kumar, A. Bhandari, P. P. Patil, “Simulation of the quadcopter dynamics with LQR based control,” *Materials Today: Proceedings*, vol. 24, pp. 326-332, 2020.

[17] H. Maghfiroh, M. Gunawan, M. Anwar, “Optimal energy control of DC-drive conveyor using LQR method,” AIP Conference Proceedings, 2217(1), pp. 030145, 2020.

[18] S. Masroor, C. Peng, A. A. Ali, M. Aamir, "Network-Based Speed Synchronization Control in the Brush DC Motors Via LQR and Multi-agent Consensus Scheme,” *Wireless Personal Communications*, 106(4), pp. 1701-1718, 2019.

[19] J. Bharti, G. Phadke, D. Patil, “Optimization of DC Motor Speed Control Using LQR Technique,” International Conference on Data Science, Machine learning & Applications, 29-30 May 2019, Hyderabad, India, pp. 1492-1499, 2020.

[20] M. Sharma, “A review on DC motor speed control using artificial neural network,” *International Journal of Engineering, Science and Mathematics*, 7(8), pp. 27-33, 2018.

[21] M. A. Aravind, N. S. Dinesh, K. Rajanna, “Application of EMPC for precise position control of DC-motor system with Backlash,” *Control Engineering Practice*, vol. 100, pp. 104422, 2020.

[22] H. Patel, H. Chandwani, “Simulation and experimental verification of modified sinusoidal pulse width modulation technique for torque ripple attenuation in Brushless DC motor drive,” *Engineering Science and Technology, an International Journal*, 24(3), pp. 671-681, 2021.

[23] R. Isermann, J. Schaffnit, S. Sinsel, “Hardware-in-the-loop simulation for the design and testing of engine-control systems,” *Control Engineering Practice*, 7(5), pp. 643-653, 1999.

[24] A. A. Hagras, “Nonlinear adaptive extended state space predictive control of permanent magnet synchronous motor,” *International Transactions on Electrical Energy Systems*, 29(1), pp. e2677, 2019.

[25] B. H. Nguyen, M. P. Cu, M. T. Nguyen, M. S. Tran, H. C. Tran, “LQR and fuzzy control for reaction wheel inverted pendulum model,” *Robotica & Management*, 24(1), pp. 19-23, 2019.

[26] S. Masroor, C. Peng, Z. A. Ali, "Event-triggered multi-agent consensus of DC motors to regulate speed by LQR scheme," *Mathematical and Computational Applications*, 22(1), pp. 14, 2017.

[27] A. Owczarkowski, D. Horla, J. Zietkiewicz, “Introduction of feedback linearization to robust LQR and LQI control–analysis of results from an unmanned bicycle robot with reaction wheel,” *Asian Journal of Control*, 21(2), pp. 1028-1040, 2019.

[28] S. S. Sankeshwari, R. H. Chille, “Performance Analysis of Disturbance Estimation Techniques for Robust Position Control of DC Motor,” *International Journal of Control, Automation, and Systems*, 18(2), pp. 486-494, 2020.

[29] N. Kumar, J. Ohri, “Novel m-PSO optimized LQR control design for Flexible Link Manipulator: An experimental validation. Majlesi," *Journal of Electrical Engineering*, 14(2), pp. 81-92, 2020.

[30] P. C. Eze, "An Enhanced PID Control Technique for Mobile Satellite Dish Antenna Network within Nigeria. Journal of Electrical Engineering, Electronics," *Control and Computer Science*, 6(3), pp. 25-30, 2020.

[31] S.O. Madbouly, A. M. Sharaf, "A novel regulation inter-coupled control scheme for a doubly-fed wind induction system," *Turkish Journal of Electromechanics and Energy*, 1(2), pp. 8-16, 2016.

[32] I. A. Aden, H. Kahveci, M. E. Şahin, "Single input, multiple output DC-DC buck converter for electric vehicles," *Turkish Journal of Electromechanics & Energy*, 2(2), pp. 7-13, 2017.

[33] A. Boztaş, O. Demirbaş, & M. E. Şahin, "Investigation of vertical axis wind turbines and the design of their components," *Turkish Journal of Electromechanics and Energy*, 6(2), pp. 64-72, 2021.

[34] K. J. Åström, T. Hägglund, K. J. Astrom, "Advanced PID control," Research *Triangle Park: ISA-The Instrumentation, Systems, and Automation Society*, vol. 461, 2006.

Biography

Ömer Kasım received his B.E. degree in Computer Engineering from Kütayha Dumlupınar University, Kütahya and received his M.E. and Ph.D. degree in electronics and computer teaching from Marmara University, İstanbul. He is currently working towards a Ph.D. degree in Electrical and Electronics Engineering at Kütahya Dumlupınar University, Kütahya. He has five years of teaching experience at Electrical and Electronics Engineering at Simav Technology Faculty. He published around 20 papers in reputed National/International journals like Elsevier, Springer, Taylor and Francis, etc., indexed in SCI, SCIE, ESCI, Scopus & Web of Science. He presented 15 papers at National/International conferences. His research interest includes artificial intelligence, biomedical engineering, mechatronics and cyber security.

E-mail: omer.kasim@dpu.edu.tr